Volume 21
Number 7
7 April 2021
Pages 1189–1420

Lab on a Chip

Devices and applications at the micro- and nanoscale

rsc.li/loc

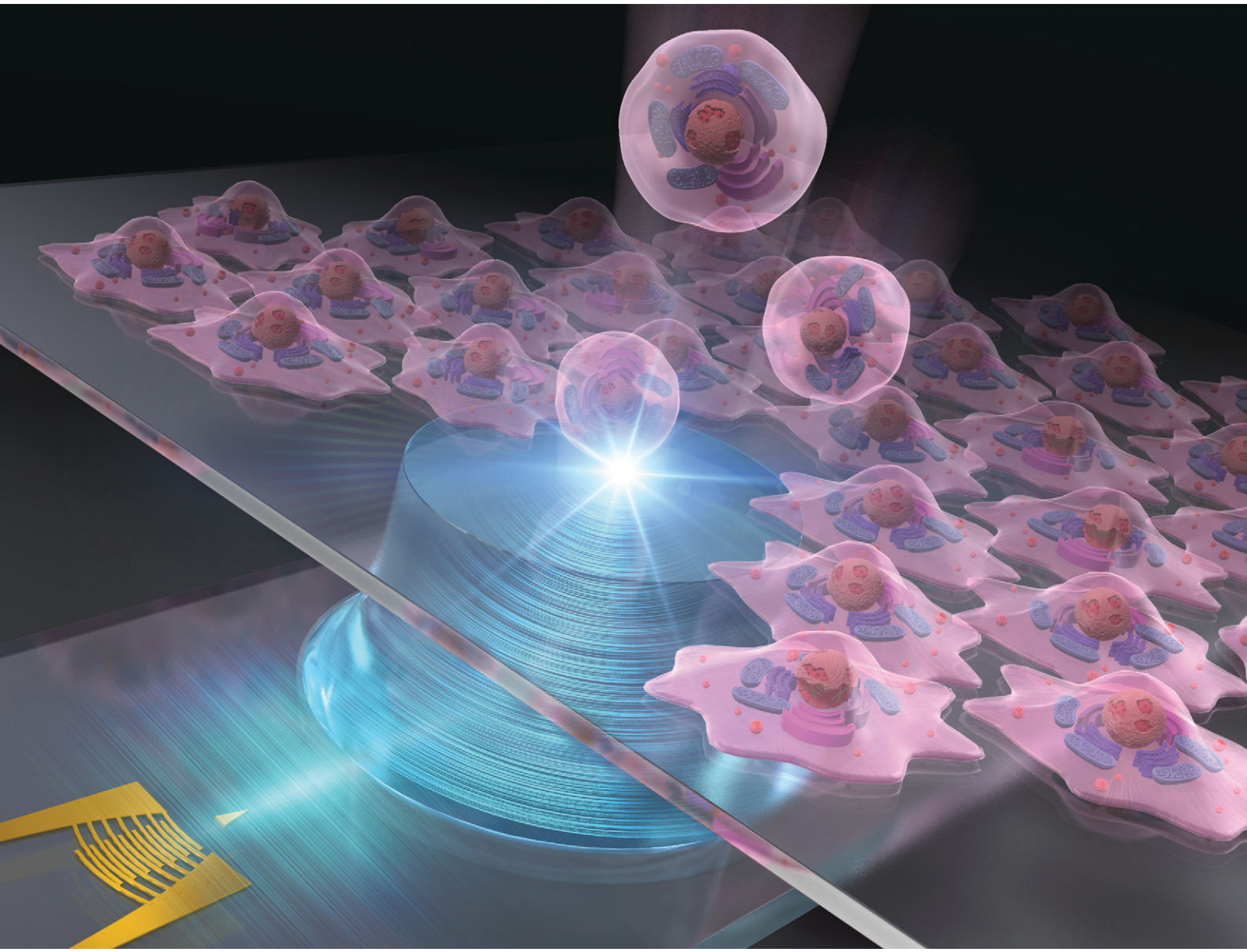

ISSN 1473-0197

ROYAL SOCIETY OF CHEMISTRY

PAPER
Kenjiro Takemura *et al.*
Focused surface acoustic wave locally removes cells from culture surface

Lab on a Chip

PAPER

View Article Online
View Journal | View Issue

Cite this: *Lab Chip*, 2021, **21**, 1299

Focused surface acoustic wave locally removes cells from culture surface

Takumi Inui,[a] Jiyang Mei,[b] Chikahiro Imashiro,[ac] Yuta Kurashina,[d] James Friend [b] and Kenjiro Takemura [*a]

Regenerative medicine and drug development require large numbers of high-quality cells, usually delivered from *in vitro* culturing. During culturing, the appearance of unwanted cells and an inability to remove them without damaging or losing most if not all the surrounding cells in the culture reduce the overall quality of the cultured cells. This is a key problem in cell culturing, as is the inability to sample cells from a culture as desired to verify the quality of the culture. Here, we report a method to locally remove cells from an adherent cell culture using a 100.4 MHz focused surface acoustic wave (SAW) device. After exposing a plated C2C12 mouse myoblast cell culture to phosphate buffered solution (PBS), ultrasound from the SAW device transmitted into the cell culture *via* a coupling water droplet serves to detach a small grouping of cells. The cells are removed from an area 6×10^{-3} mm^2, equivalent to about 12 cells, using a SAW device-Petri dish water gap of 1.5 mm, a PBS immersion time of 300 s, and an input voltage of 75 V to the SAW device. Cells were released as desired 90% of the time, releasing the cells from the target area nine times out of ten runs. In the one trial in ten that fails, the cells partially release and remain attached due to inter-cellular binding. By making it possible to target and remove small groups of cells as desired, the quality of cell culturing may be significantly improved. The small group of cells may be considered a colony of iPS cells. This targeted cell removal method may facilitate sustainable, contamination-free, and automated refinement of cultured cells.

Received 21st December 2020,
Accepted 3rd March 2021

DOI: 10.1039/d0lc01293a

rsc.li/loc

1 Introduction

Regenerative medicine, reliant on cell culturing, promises to ease the financial and social burden of rapidly aging societies.[1,2] However, the tissue and organs to be generated and regenerated to achieve this promise requires, at its core, high-quality, pure, and numerous cells to be rapidly cultured. Tissues and cells produced in this way are also a promising alternative to animal experiments during drug discovery and testing.[3,4] While the culturing of cells is a classic process in biology and medicine, as medical practitioners and biologists continue to devise ever more beneficial applications of this process, engineers must act to improve its speed, quality, and stability.[5]

With automation, one of the most important requirements for mass cell culture is quality control.[6,7] As living cells have potentially significant differences between them as they reproduce, either from differentiation or mutation, the appearance of local colonies of unwanted cells in a monolithic culture is a common and difficult challenge. Such cell aggregations or dense cell monolayers during cell culture may induce cell inactivation or unexpected differentiation.[8] Undifferentiated induced pluripotent stem (iPS) cells or cells differentiated to a different lineage from the desired one may result in tumor formation when implanted into a patient.[9,10] There are essentially two methods to remove unwanted cells: chemical and physical. Tohyama *et al.* removed undifferentiated iPS cells possibly appearing in cardiomyocytes differentiated from iPS cells by exploiting the difference in metabolic characteristics between them.[11] They introduced a lactic acid-laden medium into the culture vessel in which only the differentiated cardiomyocytes could survive. The purity of cardiomyocytes was 98.7% after the treatment. Unfortunately, about 1% of the culture was still undifferentiated iPS cells. While this purity may be higher than encountered in our body, it still remains a problem in a generated culture intended for implantation.

[a] *Department of Mechanical Engineering, Keio University, Yokohama 223-8522, Japan. E-mail: takemura@mech.keio.ac.jp; Fax: +81 45 566 1826; Tel: +81 45 566 1826*
[b] *Medically Advanced Devices Laboratory, Center for Medical Devices, Department of Mechanical and Aerospace Engineering, Jacobs School of Engineering, Department of Surgery, School of Medicine, University of California San Diego, CA 92093, USA*
[c] *Institute of Advanced Biomedical Engineering and Science, Tokyo Women's Medical University, TWIns, Tokyo 162-8666, Japan*
[d] *Department of Materials Science and Engineering, Tokyo Institute of Technology, Yokohama 226-8503, Japan*

Fluorescence-activated cell sorting (FACS) is another option for isolating unwanted cells.[12,13] Cells fluorescently labelled with an antibody are sorted. However, cells must be released from adhesion during culturing to perform FACS, which reduces the quality of the cells due to the (trypsin) detachment and subsequent reseeding of the cells after sorting.[14,15] It also increases the risk of contamination from antibody labeling and the added handling. Edahiro *et al.* selectively removed cells by using a photoresponsive culture substrate.[16] The light reduces the adhesion between the culture surface and cell, causing cell release. This method is promising but requires a specially coated culture surface different from those widely used in bioengineering. The authors have developed a method to locally remove cells using a kHz-order ultrasonic, conical horn from a standard culture dish,[17] demonstrating that ultrasonic irradiation is effective in releasing cells from attachment. However, because the cell release area is large at 0.1 mm^2, representing about 200 cells on average in a monolayer culture, it cannot be said to be a "local" cell removal method. iPS cells exist in a colony on a culture surface in order to proliferate even when the cells are not confluent in a culture vessel.[18] From this viewpoint, removing a group of ~10 cells is a reasonable target as a "local" removal of cells.

In order to release cells in a much smaller, local region at will from a standard culture dish, this study employs a focused SAW device capable of applying a large pressure to a much smaller circular region, a size approaching the diameter of individual cells adherent on a culture surface. Beyond the benefit of the relatively small size of the detachment location, the SAW device is far smaller, more easily manipulated, and produces a much more focused acoustic wave than an ultrasonic horn. In what follows, we identify the aspects of this method that are most important to consider in using it for targeted cell detachment, and evaluate the viability of the released cells after exposure to the SAW-driven acoustic wave.

2 Materials and methods

2.1 Cell release concept

The concept of locally removing cells from a culture surface by using focused SAW is illustrated in Fig. 1a. The SAW generated by a concentric arc interdigital transducer (IDT) (see Fig. 1d) propagates on a piezoelectric substrate ($LiNbO_3$ for example), and focuses at the focal point where a water droplet (ultrasonic couplet between the SAW device and a cell culture dish) is placed. Once the SAW reaches the water droplet (Fig. 1b), the ultrasonic longitudinal wave propagates into water at the Rayleigh angle

$$\theta_R = \sin^{-1}\left(\frac{c_w}{c_s}\right) \quad (1)$$

where c_w (= 1480 m s^{-1}) and c_s (= 3790 m s^{-1}) are the sound speeds of a longitudinal wave in water and SAW upon a $LiNbO_3$ piezoelectric substrate. At the boundary between

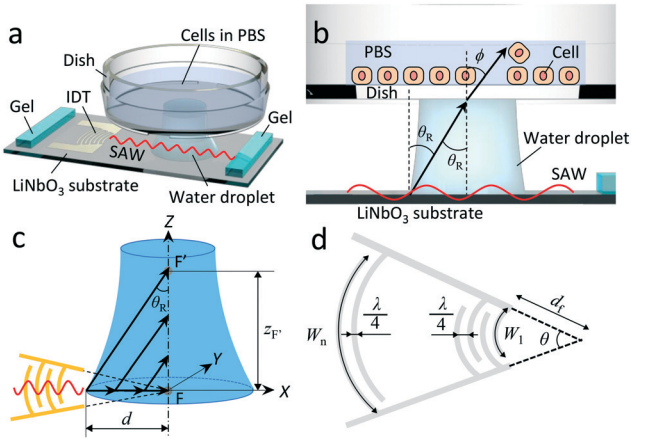

Fig. 1 Locally removing cells from a culture surface by using focused SAW. (a) Conceptual illustration. (b) Ultrasonic longitudinal vibration propagates into the dish at the Rayleigh angle, θ_R, and the refractive angle, ϕ. (c) An ultrasonic longitudinal wave converges along the vertical line. (d) Schematic diagram of concentric IDT.

water and the polystyrene dish, the wave deflects according to Snell's law at the refractive angle[19] defined as

$$\phi = \sin^{-1}\left(\frac{c_d \sin\theta_R}{c_w}\right) \quad (2)$$

where, c_d (= 2340 m s^{-1}) is the sound speed of a longitudinal wave in polystyrene. Since the Rayleigh angle θ_R and the refractive angle ϕ are 23° and 38° according to eqn (1) and (2), we may conclude the ultrasonic longitudinal wave will propagate into the dish without total reflection as illustrated in Fig. 1b. Cells located in the path of the ultrasonic longitudinal wave will be exposed to an ultrasonic radiation force.[20,21]

The converging nature of ultrasound generated in the coupling water droplet from the focused SAW device is illustrated in Fig. 1c. As the SAW reaches the edge of the water droplet, it is progressively reduced in amplitude as the energy of the SAW in the substrate is "leaked" into the water to produce longitudinally oriented sound at the Rayleigh angle. This attenuation of the SAW in the substrate is rapid and distinct from the attenuation of the sound propagating in the fluid.[22] At 100 MHz, the SAW propagation on the $LiNbO_3$ substrate is attenuated to a negligible amplitude over only 500 μm, while the sound formed in the fluid may propagate 5 mm. This forms a 500 μm deep—along the *X* axis—beam of ultrasound propagating upwards in the coupling fluid at the Rayleigh angle toward the point *F*′.

While the SAW produces an acoustic beam only 500 μm wide along the *X* axis direction, the SAW may still have a significant width along the *Y* axis direction if the fluid is present closer to the IDT than the IDT's focal point defined at *F*. In other words, even if the SAW will be absorbed before reaching to the focal point, *F*, due to the fluid existing on the $LiNbO_3$ substrate, an acoustic wave that is 500 μm wide along *X* but wider along *Y* will be produced in the fluid. Nonetheless, the focusing of the acoustic wave in the fluid

couplant drop continues towards F', as the drop has a curved contact line nearest the IDT, and the incident SAW is propagating inwards toward a focus (F) it will never reach when it encounters the drop's contact line.

Because the shape of the couplant drop is not defined beforehand, it is difficult to precisely define, in advance, the location of F'. However, it is possible to identify its location *via* experiment, and with good repeatability. This may be used to determine the appropriate gap between the substrate and the dish in order to facilitate focused, localized cell removal (see section 3).

2.2 Focused SAW device

Fig. 1d illustrates the concentric arc IDT patterned on a standard 0.5 mm thick, 127.68° Y-rotated, X-propagating $LiNbO_3$ substrate (Roditi, London, UK). In the figure, λ, d_f, θ, n, and W_n represent the SAW's wavelength and the focal distance, focusing angle, number of finger pairs, and aperture for electrode n of the IDT, respectively. Note that the wavelength is defined as $\lambda = \frac{C_s}{f}$, where f is the selected driving frequency. Since the aperture may be calculated as

$$W_n = \left(\frac{d_f + (4n - 3)}{8}\right)\theta, \quad (3)$$

the focal diameter of the focused SAW, D, may be defined as the region within −4 dB of maximum amplitude[23] and is

$$D = \frac{\lambda d_f}{W_n}. \quad (4)$$

In this study, we chose f = 100 MHz (*i.e.*, λ = 39.8 μm), d_f = 522 μm, $\theta = \pi/3$, and n = 48 for the design of our SAW device as exemplified in Fig. 2a. With these parameters, the focal diameter D is 13.5 μm according to eqn (4).

A 400 nm thick aluminum IDT was patterned on our $LiNbO_3$ substrate using liftoff photolithography.[24] The triangular pattern on the substrate is a conductive waveguide to effectively focus the SAW.[25] The S11 parameter of the SAW device was measured using a network analyzer (E5061B, Keysight, CA, USA) to be −2.51 dB. Applying a 50 $V_{0\text{–}p}$ sinusoidal signal to the bus bars of the IDT, we characterized the developed SAW device by a laser Doppler vibrometer (CLV-3000, Polytech, Germany).

2.3 Concept verification by removing particles using a focused SAW device

In order to verify our concept, we initially demonstrated the removal of particles from a culture dish by using the focused SAW device. The experimental setup was simply constructed as shown in Fig. 2b. The SAW device is placed atop a vibration absorbing gel pad (D-180, Daiso-sangyo, Hiroshima, Japan) and a ϕ 35 mm diameter cell culture dish (150 460, ThermoFisher Scientific Co., MA USA), with a gap between the latter two items. This culture dish is used for all

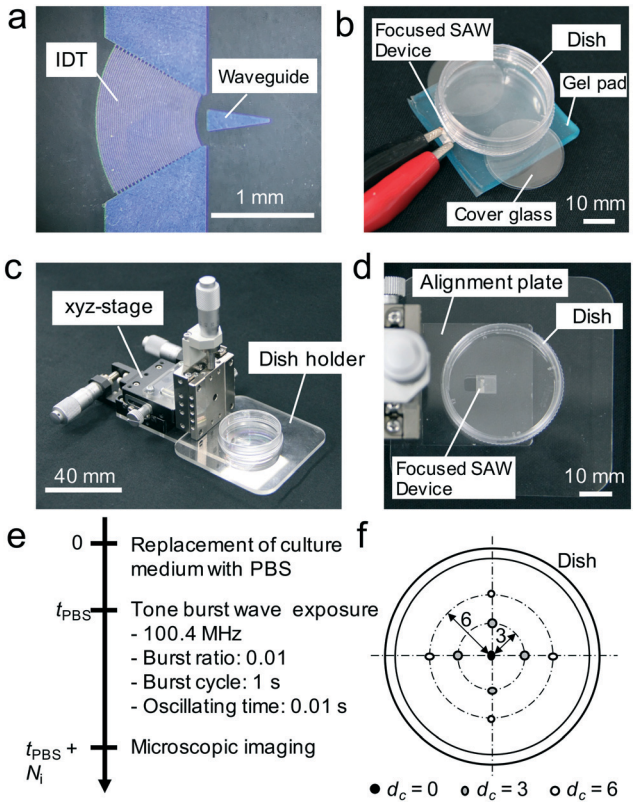

Fig. 2 Fabricated SAW device and experimental setup. (a) Fabricated SAW device with waveguide. (b) Setup for particle removing experiment. (c) Cell removing system. (d) Arrangement of the SAW device and adherent cell culture dish. (e) Timeline of our standard experimental procedure. (f) Ultrasonic longitudinal wave irradiation positions indicated with circles. d_c represents the distance from dish center.

experiments in this study. The gap was adjusted to 0.2 mm by stacking two 0.1 mm thick, ϕ 18 mm cover glass pieces (C018001, Matsunami Glass Ind., Ltd., Osaka, Japan) between the dish and the gel pad. On the dish surface, we introduced apatite particles (Ag Deo, Shiseido Co. Ltd., Tokyo, Japan) and pipetted 1 mL water into the dish. Applying 100.4 MHz, 100 V sinusoidal input to the bus bars of the SAW device, we observed the removal of particles from the surface at the focal point. Note that employing apatite particles is a reasonable choice to show the propagation even without input parameters optimization, since the adhesion between dish and apatite particles is not strong.

2.4 Cell preparation

A mouse myoblast cell line, C2C12 (RCB0987, RIKEN BRC, Japan), widely used in biomedical research,[26,27] was employed in this study to represent typical adherent cells. The cells were seeded onto a culture dish and incubated with culture medium (Dulbecco's Modified Eagle's Medium/ Nutrient Mixture + 10% FBS SA, SigmaAldrich, MO USA) in CO_2 5% humidified incubator (CPE-2601, Hirasawa Co., Japan) at 37 °C. Then these cells were subcultured with

Trypsin–EDTA (0.05%) (ThermoFisher Scientific Co., MA USA) until cells reached visual confluence (approximately 1.2×10^6 cells). When preparing a sample for a cell removal experiment, 5.0×10^5 cells were seeded into the culture dish and incubated for 24 h before the experiment.

In addition, the 24 h cultured cell nuclei were stained with Hoechst 33342 (H1399, Thermo Fisher Scientific Co.) in order to aid determination of the number of cells per unit area *via* fluorescent microscopy (ECLIPSE Ti–S, Nikon Co., Japan). Fluorescent images of cell nuclei were analyzed with ImageJ (Ver1.50i, NIH, USA) to calculate the cell density on the culture dish.

2.5 Cell detachment system and experimental procedure

A cell detachment system was fabricated as shown in Fig. 2c and d. The system consists of the focused SAW device placed on an alignment plate, a 35 mm diameter culture dish affixed to a dish holder, and an xyz-stage (XYCRS120/ZLPG80, MISUMI Co., Japan) to position the culture dish with regard to the focused SAW device. The arrangement was placed on a phase contrast microscope (ECLIPSE Ti–S, Nikon Co., Japan) *via* a specialized jig which enables the alignment of the coordinate systems of the stage and the microscope. By doing so, the positions where the ultrasonic wave was introduced could be directly correlated to where the cells were removed.

A standard cell-release experiment is shown in Fig. 2e. First, adherent cells on the culture dish were exposed to phosphate-buffered saline (PBS) over time, t_{PBS} to weaken the cell adhesion.[28] The dish with these cells was then placed into the cell release system, and SAW was used to expose cells in five regions to ultrasound (see Fig. 2f) while employing different gap lengths, G, between the SAW device and the culture dish. Instead of continuous exposure, we employed a burst signal for the SAW device, produced *via* a function synthesizer (WF1946B, NF Co., Japan) and an amplifier (LZY-22+, Mini-Circuits, USA). The burst ratio, burst cycle, and oscillating time were set to 0.01, 1 s, and 0.01 s, respectively. This reduces the risk of adverse heating of the cells. The SAW exposure time, defined in terms of the number of burst cycles the cells were irradiated with ultrasound, N_i, was varied. For example, setting $N_i = 1$ produces a single exposure of the cells to ultrasound of 0.01 s. Setting $N_i = 10$ implies ten such exposures individually spaced in time by 0.99 s.

The driving frequency of the SAW device was fixed to 100.4 MHz, corresponding to the resonance, but the input voltage, V_{in}, was changed. Using phase contrast microscope images of the exposed region after ultrasound exposure, we determined the area of the region from which cells were released using ImageJ. We employed four distinct culture dishes for each experiment, and so twenty data points were captured for each combination of parameters in this experiment.

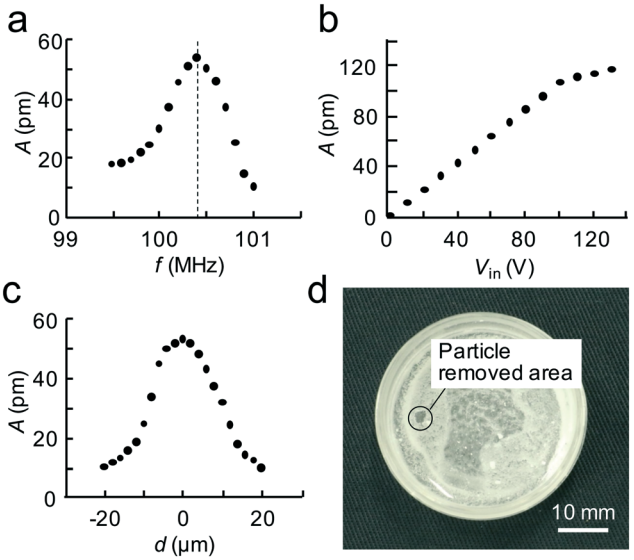

Fig. 3 Fundamental experimental results. (a–c) Characteristics of the fabricated SAW device. (a) Relationship between input frequency, f, and vibration amplitude, A. The fabricated SAW device resonates at 100.4 MHz. (b) Relationship between input voltage, V, and vibration amplitude, A. The vibration amplitude of the SAW device is almost linear up to 100 V. (c) Relationship between the distance, d, from the focal point, F, and the vibration amplitude, A. The focal diameter of the fabricated SAW device at F is estimated to be 15.1 μm. (d) Particle removal experiment. Apatite particles were locally removed from the dish surface with 100.4 MHz ultrasonic irradiation generated with 100 V input to the SAW device. This shows the acoustic wave successfully propagate to the dish.

3 Results and discussion

3.1 Experiments exploring the concept

Fig. 3a indicates the fabricated SAW device resonates at 100.4 MHz. The relation between the voltage (zero-peak) and the maximum amplitude (peak–peak) at the focal point at a driving frequency of 100.4 MHz is almost linear up to 100 V input, as shown in Fig. 3b. The actual focal diameter of the ultrasound at the focal point F from the SAW device, defined as the region where the ultrasound is within 4 dB of the maximum amplitude, is 15.1 μm according to the results in Fig. 3c, which shows the amplitude distribution with regard to the distance from the focal point, F. Note that this compares favorably to the expected focal diameter of 13.5 μm from the design (see 2.2).

Fig. 3d shows apatite particle removal by ultrasound from the focused SAW at a driving frequency of 100.4 MHz and a voltage of 100 V. As can be seen, particles were removed from a 2 mm diameter area. The key result from the particle removing experiment is the ability to transmit focused SAW as ultrasound to a point on the dish surface which subsequently acts to displace particles in a small region at this point.

3.2 Targeted adherent cell release

Fig. 4a shows the stained cell nuclei under fluorescent imaging obtained for confirming the adherent cell density

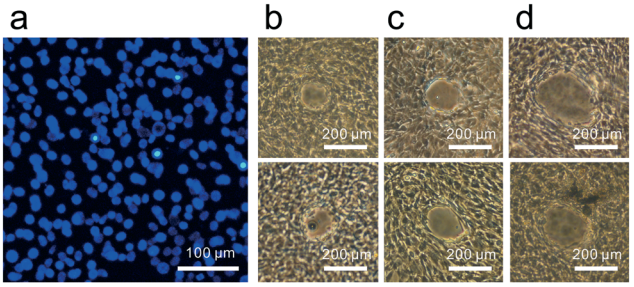

Fig. 4 Actual cell images. (a) Fluorescent image of cell nuclei. From this image, the cell density before the detachment experiment was estimated to be 2.06×10^{-3} cells per μm^2. (b–d) Representative regions where cells were removed using the focusing SAW-driven ultrasound, with G = 1.5 mm, N_i = 1, V_{in} = 50 V, and (b) t_{PBS} = 0 s, (c) t_{PBS} = 300 s, or (d) t_{PBS} = 600 s.

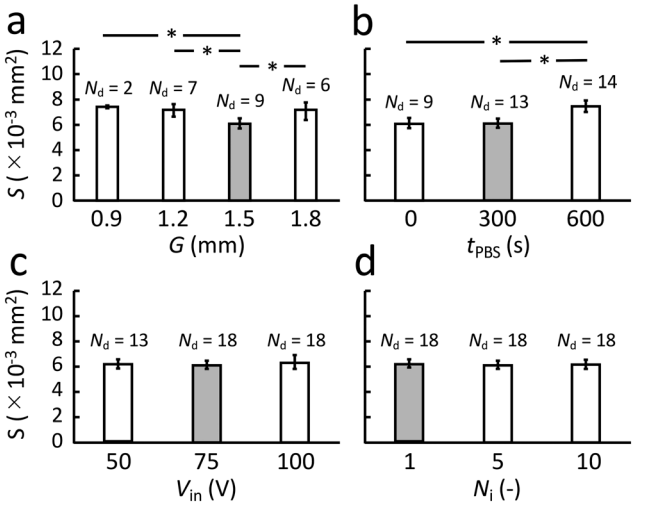

Fig. 5 Effect of each parameter on cell release region's area, S. N_d indicates the number of trials that successfully produced cell release from the ultrasound exposed region out of a total of 20 trials. The gray filled bars represent the overall best result for each case; when there is an insignificant difference between two choices, the lower energy, lower exposure choice is always selected. (a) Gap, G, between the SAW device and dish was changed while t_{PBS} = 0 s, N_i = 1, V_{in} = 50 V were kept constant. (b) PBS immersion time, t_{PBS}, was changed while G = 1.5 mm, N_i = 1, V_{in} = 50 V were kept constant. (c) The input voltage was changed, while G = 1.5 mm, t_{PBS} = 300 s, and N_i = 1 were kept constant. (d) The number of exposure cycles was changed while G = 1.5 mm, t_{PBS} = 300 s, V_{in} = 75 V were kept constant. The total number of trials in each case was n = 20, mean $\pm$ $^{max}_{min}$, *: $p < 0.05$. As results of parametric investigations against each parameter, G, t_{PBS}, V_{in}, and N_i, we concluded the best combination for the current setup is G = 1.5 mm, t_{PBS} = 300 s, V_{in} = 75 V, and N_i = 1.

prior cell release experiments. From an average of three such images, the adherent cell density was estimated to be 2.06×10^{-3} cells per μm^2. Fig. 4b–d provide representative images of cell release from an adherent cell culture in the culture dish as obtained *via* phase contrast microscopy when the PBS immersion time was varied. As mentioned in section 2.1, four parameters are to be investigated in the experiments. The gap, G, between SAW device and culture dish is first investigated as the geometric parameter for the setup. Second, the PBS immersion time, t_{PBS}, is varied since it has been revealed in advance from our earlier work that we cannot reliably detach cells without the help of PBS.[20] Variations of the input voltage, V_{in}, and the number of ultrasound exposure cycles, N_i, are then carried out.

3.2.1 Effect of the gap, G, between SAW device and culture dish. The sole geometric parameter under consideration in this study is the gap distance, G, between the SAW device and the culture dish. Changing the gap to be either G = 0.9, 1.2, 1.5, or 1.8 mm produces significant changes in the cell release region's area, S, as shown in Fig. 5a. The other parameters were held constant at t_{PBS} = 0 s (cells remained immersed in growth media), N_i = 1, and V_{in} = 50 V. N_d in the figure indicates the number of exposure points where we could observe cell removal out of 20 points in total. Recall that N_i = 1 is a single ultrasound exposure of 0.01 s.

From the figure, we can conclude that a gap G = 1.5 mm appears best since it produces the smallest detachment area with the highest rate of success, N_d, at 9/20 under these specific conditions. Compare this result to a simple estimate of the location of the point, F', as follows, referring to Fig. 1,

$$G = z_{F'} = \frac{d}{\tan \theta_R} \approx 1.2 \text{ mm}. \quad (5)$$

This approximation does not take into account the glass over part of the ultrasound's propagation, but is still reasonably close to the experimentally determined value. Irrespective of this estimate, it is clear from the results that the gap is indeed important in obtaining focused and reliable cell release.

3.2.2 Effect of the PBS immersion time, t_{PBS}. The PBS immersion time, t_{PBS} was next investigated by varying it from 0 to 300 and 600 s. The other parameters were fixed at G = 1.5 mm, N_i = 1, and V_{in} = 50 V. As the PBS immersion time increases, both the success rate, N_d, and the area of cell release, S, increased as indicated in Fig. 5b. Since N_d increased significantly as t_{PBS} was increased from 0 to 300 s, we may conclude that exposure to PBS prior to adherent cell exposure to the SAW-driven ultrasound is important to improving this method's success rate. Such exposure, however, does not appear to significantly increase the cell release area, S. A careful reader will recall from Fig. 4 that increasing t_{PBS} does—however—visibly increase the size of the cell release area. Curiously, this effect is especially pronounced as t_{PBS} is increased from 300 to 600 s, and is statistically significant as indicated in Fig. 5b. By contrast, the number of successful cell release events is only slightly improved, from N_d = 13 to N_d = 14, when increasing t_{PBS} from 300 s to 600 s. This interesting result may be based on the following hypothesis. In the present experiment, cells form a confluent cell monolayer on the culture surface, where the effect of PBS is likely to progress from the top of the cells to the bottom due to diffusion. This is supported by past observations in cultured cells to produce tissue.[29,30] While cell-culture surface adhesions appear deeply within the cell

monolayer, inter-cellular bindings tend to be located near the top surface of the cell monolayer. Thus, we may predict that PBS will first affect the inter-cellular binding and later affect the cell-culture surface adhesion; t_{PBS} = 300 s may be long enough to weaken the inter-cellular binding to get a higher success rate. However, t_{PBS} = 600 s is too long, producing a larger cell release area due to the reduced cell adhesion induced by the diffusion of the PBS into the cell-culture surface. Based upon the results shown in Fig. 5b, we adopted t_{PBS} = 300 s for the following experiments.

3.2.3 Effect of the input voltage, V_{in}. The input voltage into the SAW device directly affects the ultrasonic radiation pressure the cells experience,[20,31] and could therefore be expected to significantly affect both the success rate and size of cell release. However, as indicated in Fig. 5c, the input voltage does not significantly affect the cell release area. There is an improvement in the cell release success rate from N_d = 13 to N_d = 18 with an increase in the applied voltage from 50 to 75 V, but this improvement does not change as the voltage is further increased to 100 V. For these trials, G = 1.5 mm, t_{PBS} = 300 s, and N_i = 1 were held constant. As before, since 75 V is the minimum voltage choice we considered that was equally successful with the higher voltage alternative, we selected it for subsequent experiments.

3.2.4 Effect from the number of ultrasound exposure cycles, N_i. The last parameter to be considered in this study was the number of ultrasound exposure cycles, N_i. Holding the other parameters constant at G = 1.5 mm, t_{PBS} = 300 s, and V_{in} = 75 V, Fig. 5d indicates both the number of successful trials, N_d out of 20 total, and the cell release area, S. These results indicate, remarkably, that changing the number of exposure cycles has no significant effect on either the success rate or the release area.

3.2.5 Strategies to improve the success rate of cell release. The success rate of removing cells is 90% with our method, at least with C2C12 cells. The question here is why we cannot always remove cells. The reason must be due to the variability of cell adhesion morphology during culture. Since the cells may migrate on a culture surface, the cell adhesion strength always varies. In addition, the stage of cell development may play an important role in the cell adhesion. During the M period, in which a cell is dividing, cell adhesion is relatively weak.[32] These adhesion strength variations are strongly related to the deformation of cells.[33] If the cell detachment treatment is conducted during medium replacement, the failure rate would be reduced to 0.1^n with n treatments. Since our proposed method requires cells be immersed in PBS, the cell detachment treatment is suitable when the medium replacement procedure takes place, because, in general, cells are washed with PBS during the medium replacement procedure. This may increase the reliability of the purification of cells. Another possible solution to overcome this limitation is to use a higher frequency transducer, because the cells are supposed to be removed by acoustic radiation pressure or possibly acoustic pressure (*c.f.* section 3.3), which are both proportional to the frequency of the ultrasonic wave. However, this increases the possibility of cell damage through heating, not only to the released cells but also to those cells left behind that are adjacent the release region. A final option may be to expose the release region to additional bursts of SAW at higher voltages. While this did not appear to substantially affect the results of our experiments in Fig. 5, it is important to note that these results were obtained from sequentially testing 20 regions without later returning to those regions that failed to release cells for additional exposure.

3.3 Effect of the ultrasound exposure position

The overall vibration of the culture dish could be an important factor in the observed behavior. While the ultrasound certainly passes through the dish, causing the generation of what is likely a Lamb wave to carry the energy across it, there may be modal conversion to produce more significant dish vibration that could be responsible for the observed cell detachment phenomena. If this were the case, the cell release capability would depend upon the position of the ultrasound emission from the SAW device.

However, there is no significant difference between points selected for cell release from the center of the dish (d_c = 0) to d_c = 3 mm and d_c = 6 mm from the dish center as indicated in Fig. 6. There is furthermore no significant difference in the area of the cell release region, S, between these points. Finally, the offset, e_p, between the predicted position of the ultrasound focus, F', and the actual cell release location is statistically identical regardless of the point chosen on the dish to release cells. If the dish were a significant part of the physical phenomena of the ultrasonic cell release, one would expect a significant difference in any or all of these aspects. Instead, it appears the observed cell release phenomena is due to the localized effects of the ultrasound propagation from the SAW device and through to the cell layer adherent on the dish. The experimental conditions were otherwise defined as t_{PBS} = 300 s, G = 1.5 mm, N_i = 1, and V_{in} = 75 V.

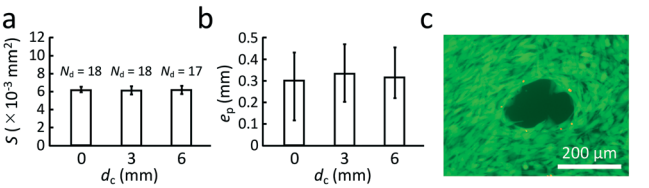

Fig. 6 Cell release with t_{PBS} = 300 s, G = 1.5 mm, N_i = 1, and V_{in} = 75 V. (a) The dependence of cell release area, S, on the position of the cell release region at a distance d_c from the center of the culture dish, with no significant differences observed. (b) Similarly, changing the position of the ultrasound exposure point has no effect upon the difference between the position of the point, F' (see Fig. 1) and the actual cell release location, $e_p \approx 300$ μm. (c) The viability of the cells left behind is generally good, with calcein stain green indicating viable cells and approximately six propidium iodide-stained red points in this typical image indicating dead cells. In each case, the number of trials n = 20, mean $\pm$ $^{max}_{min}$.

3.4 Viability of remaining cells

The viability of cells left behind and adjacent the detachment region could be a problem given the evident intensity of the ultrasound required to release the cells in the targeted region. Calcein staining was used to identify live cells (Calcein-AM solution, Dojindo Molecular Technologies, Inc., Japan) and propidium iodide staining of dead cells (Wako Pure Chemical Industries, Ltd., Japan). The experimental conditions were t_{PBS} = 300 s, G = 1.5 mm, N_i = 1, and V_{in} = 75 V, with d_c = 0 mm: the ultrasound exposure point was at the center of the dish. A fluorescent image of stained cells around a cell released region is provided in Fig. 6c. Only a few dead cells visible as red points may be observed amid the generally green, viable cells; the dead cells are at the periphery of the cell release region. This indicates that these cells have likely been destroyed through excess shear in the process of being partially released adjacent the ultrasound exposure region and yet still adherent to cells unexposed to the ultrasound.

4 Conclusions

We have proposed a method to locally remove adherent cells from a culture surface by using a focused SAW device. When we locally expose a 100.4 MHz ultrasonic wave generated from the focused SAW device onto C2C12 cells cultured on and adherent to a dish, we may remove cells from a tiny target region of about 6×10^{-3} mm^2 after exposure to PBS for 300 s followed by the SAW-driven ultrasound. The success rate of removal was 90% (18 out of 20 trials) from our experiment, and some strategies to improve this success rate were discussed.

Removal of small numbers of cells from an adherent culture is one of the most important barriers to guaranteeing the quality of the cultured cells. This is especially important in regenerative medicine where the cells are to be implanted into humans, and where the consequences of flawed cells can be serious. Our proposed method provides a possible solution to remove small numbers of undesired cells at will, for instance undifferentiated cells from human iPS cells, to control quality. In addition, the proposed method does not require any physical contact with the adherent cells nor the insertion of instruments into the cell media, reducing the risk of contamination and cell damage. This approach may produce a sustainable, automated, and contamination-free method to refine cell cultures consistent with the needs of medicine and biology today and into the future.

The design of the SAW device is quite flexible. Here we have simply demonstrated that the focused SAW is effective in locally removing cells; however, the optimization of SAW device design, introducing additional techniques such as superposition of waves may enhance the ability and design possibilities of this method in the future.

Author contributions

TI, JRF and KT designed the study. TI, JM, CI and YK fabricated the system. TI, JM, CI and YK conducted experiments and assays. CI, YK, JRF and KT wrote the manuscript with input from all authors.

Conflicts of interest

There are no conflicts to declare.

Acknowledgements

Funding for this work conducted in Japan was provided in part from a JSPS KAKENHI (Grant Number 17KK0119 to KT, 17H07081 to YK and 20J00337 to CI). Support for the work conducted in the US was graciously provided by the W. M. Keck Foundation *via* a SERF grant to JRF.

References

1 C. Qi, L. Xu, Y. Deng, G. Wang, Z. Wang and L. Wang, *Biomater. Sci.*, 2018, **6**, 2859–2870.
2 S. Harper, *Science*, 2014, **346**, 587–591.
3 V. S. Nirmalanandhan and G. S. Sittampalam, *J. Biomol. Screening*, 2009, **14**, 755–768.
4 Y. Terao, Y. Kurashina, S. Tohyama, Y. Fukuma, K. Fukuda, J. Fujita and K. Takemura, *Sci. Rep.*, 2019, **9**, 15655.
5 D. S. Kim, M. W. Lee, Y. J. Ko, Y. H. Chun, H. J. Kim, K. W. Sung, H. H. Koo and K. H. Yo, *Cell Biochem. Funct.*, 2016, **34**, 16–24.
6 I. Horiguchi and M. Kino-oka, *Engineering*, 2021, DOI: 10.1016/j.eng.2021.01.001, Available online.
7 T. Kikuchi, M. Kino-oka, M. Wada, T. Kobayashi, M. Kato, S. Takeda, H. Kubo, T. Ogawa, H. Sunayama, K. Tanimoto, M. Mizutani, T. Shimizu and T. Okano, *Regen. Ther.*, 2018, **9**, 89–99.
8 D. S. Kim, M. W. Lee, Y. J. Ko, Y. H. Chun, H. J. Kim, K. W. Sung, H. H. Koo and K. H. Yo, *Cell Biochem. Funct.*, 2016, **34**, 16–24.
9 K. Miura, Y. Okada, T. Aoi, A. Okada, K. Takahashi, K. Okita, M. Nakagawa, M. Koyanagi, K. Tanabe, M. Ohnuki, D. Ogawa, E. Ikeda, H. Okano and S. Yamanaka, *Nat. Biotechnol.*, 2009, **27**, 743–745.
10 H. Hentzea, P. L. Soong, S. T. Wang, B. W. Phillips, T. C. Putti and N. R. Dunn, *Stem Cell Res.*, 2009, **2**, 198–210.
11 S. Tohyama, J. Fujita, T. Hishiki, T. Matsuura, F. Hattori, R. Ohno, H. Kanazawa, T. Seki, K. Nakajima, Y. Kishino, M. Okada, A. Hirano, T. Kuroda, S. Yasuda, Y. Sato, S. Yuasa, M. Sano, M. Suematsu and K. Fukuda, *Cell Metab.*, 2016, **23**, 663–674.
12 D. Guez-Barber, S. Fanous, B. K. Harvey, Y. Zhang, E. Lehrmann, K. G. Becker, M. R. Picciotto and B. T. Hope, *J. Neurosci. Methods*, 2012, **1**, 10–18.
13 S. Fickert, J. Fiedler and R. Brenner, *Osteoarthr. Cartil.*, 2003, **11**, 790–800.
14 J. P. Revel, P. Hoch and D. Ho, *Exp. Cell Res.*, 1974, **84**, 207–218.

15 H.-L. Huang, H.-W. Hsing, T.-C. Lai, Y.-W. Chen, T.-R. Lee, H.-T. Chan, P.-C. Lyu, C.-L. Wu, Y.-C. Lu, S.-T. Lin, C.-W. Lin, C.-H. Lai, H.-T. Chang, H.-C. Chou and H.-L. Chan, *J. Biomed. Sci.*, 2010, **17**, 36.
16 J. Edahiro, K. Sumaru, Y. Tada, K. Ohi, T. Takagi, M. Kameda, T. Shinbo, T. Kanamori and Y. Yoshimi, *Biomacromolecules*, 2005, **6**, 970–974.
17 T. Inui, Y. Kurashina, C. Imashiro and K. Takemura, *Eng. Life Sci.*, 2019, **19**, 575–583.
18 E. M. Chan, S. Ratanasirintrawoot, I.-H. Park, P. D. Manos, Y.-H. Loh, H. Huo, J. D. Miller, O. Hartung, J. Rho, T. A. Ince, G. Q. Daley and T. M. Schlaeger, *Nat. Biotechnol.*, 2009, **27**, 1033–1037.
19 R. P. Hodgson, M. Tan, L. Yeo and J. Friend, *Appl. Phys. Lett.*, 2009, **94**, 024102.
20 Y. Kurashina, C. Imashiro, M. Hirano, T. Kuribara, K. Totani, K. Ohnuma, J. Friend and K. Takemura, *Commun. Biol.*, 2019, **2**, 393.
21 C. Imashiro, M. Hirano, T. Morikura, Y. Fukuma, K. Ohnuma, Y. Kurashina, S. Miyata and K. Takemura, *Sci. Rep.*, 2020, **10**, 9468.
22 M. B. Dentry, L. Y. Yeo and J. R. Friend, *Phys. Rev. E: Stat., Nonlinear, Soft Matter Phys.*, 2014, **89**, 013203.
23 J. B. Green, G. S. Kino and B. T. Khuri-Yakub, *IEEE Trans. Sonics Ultrason.*, 1983, **30**, 43–50.
24 J. Mei, N. Zhang and J. Friend, *J. Visualized Exp.*, 2020, e61013.
25 J. Mei and J. Friend, *Mech. Eng. Rev.*, 2020, **7**, 19-00402.
26 C. Imashiro, Y. Kurashina, T. Kuribara, M. Hirano, K. Totani and K. Takemura, *IEEE Trans. Biomed. Eng.*, 2019, **66**, 111–118.
27 Y. Haraguchi, T. Shimizu, T. Sasagawa, H. Sekine, K. Sakaguchi, T. Kikuchi, W. Sekine, S. Sekiya, M. Yamato, M. Umezu and T. Okano, *Nat. Protoc.*, 2012, **7**, 850–858.
28 K. Ohnuma, A. Fujiki, K. Yanagihara, S. Tachikawa, Y. Hayashi, Y. Ito, Y. Onuma, T. Chan, T. Michiue, M. K. Furue and M. Asashima, *Sci. Rep.*, 2015, **4**, 4646.
29 W. Sekine, Y. Haraguchi, T. Shimizu, A. Umezawa and T. Okano, *J. Biochips Tissue Chips*, 2011, S1:007.
30 C. Imashiro and T. Shimizu, *Int. J. Mol. Sci.*, 2021, **22**, 425.
31 Y. Kurashina, M. Hirano, C. Imashiro, K. Totani, J. Komotori and K. Takemura, *Biotechnol. Bioeng.*, 2017, **114**, 2279–2288.
32 M. C. Jones, J. Zha and M. J. Humphries, *Philos. Trans. R. Soc., B*, 2019, **374**, 20180227.
33 H. Y. Yoshikawa, T. Kawano, T. Matsuda, S. Kidoaki and M. Tanaka, *J. Phys. Chem. B*, 2013, **117**, 4081–4088.